
This is an electronic reprint of the original article.

This reprint may differ from the original in pagination and typographic detail.

Khayrudinov, V; Sorokina, A; Raj, V; Gagrani, N; Koskinen, T; Jiang, H; Tittonen, I; Jagadish, C; Tan, HH; Lipsanen, H; Haggren, T

Direct GaAs Nanowire Growth and Monolithic LightEmitting Diode Fabrication on Flexible Plastic Substrates

Published in:

Advanced Photonics Research

DOI:

[10.1002/adpr.202100311](https://doi.org/10.1002/adpr.202100311)

Published: 01/08/2022

Document Version

Publisher's PDF, also known as Version of record

Published under the following license:

CC BY

Please cite the original version:

Khayrudinov, V., Sorokina, A., Raj, V., Gagrani, N., Koskinen, T., Jiang, H., Tittonen, I., Jagadish, C., Tan, HH., Lipsanen, H., & Haggren, T. (2022). Direct GaAs Nanowire Growth and Monolithic LightEmitting Diode Fabrication on Flexible Plastic Substrates. *Advanced Photonics Research*, 3(8), Article 2100311. <https://doi.org/10.1002/adpr.202100311>

This material is protected by copyright and other intellectual property rights, and duplication or sale of all or part of any of the repository collections is not permitted, except that material may be duplicated by you for your research use or educational purposes in electronic or print form. You must obtain permission for any other use. Electronic or print copies may not be offered, whether for sale or otherwise to anyone who is not an authorised user.

Direct GaAs Nanowire Growth and Monolithic Light-Emitting Diode Fabrication on Flexible Plastic Substrates

Vladislav Khayrudinov,* Anastasiia Sorokina, Vidur Raj, Nikita Gagrani, Tomi Koskinen, Hua Jiang, Ilkka Tittonen, Chennupati Jagadish, Hark Hoe Tan, Harri Lipsanen, and Tuomas Haggren

The growth of self-catalyzed GaAs nanowires (NWs) and monolithic light-emitting diode (LED) directly on flexible plastic substrates is reported. Dense GaAs NW forest is attained in self-catalyzed mode using metalorganic vapor phase epitaxy. The NWs are shown to be crystalline with a zinc-blende phase. The optical properties of the GaAs NWs are found to be promising in both photoluminescence emission and light-trapping based on reflectance and transmittance measurements. The LED is fabricated from p-type NWs by depositing Au as Ohmic contact and TiO₂/ITO as an electron-selective contact. The demonstrated NW growth and LED fabrication represent a significant step toward low-cost, industrially feasible flexible III–V NW optoelectronic applications, as plastic is inexpensive, and the fabrication steps are compatible with roll-to-roll processing.

1. Introduction

III–V semiconductor nanowires (NWs) have been in the center of scientific attention over the last two decades thanks to a number of remarkable mechanical, optical, and electrical properties such as high carrier mobility, doping control, efficient light trapping, direct tunable bandgap, and excellent strain relaxation.^[1] In particular, GaAs NWs have been used in a myriad of applications, including solar cells, lasers, photodetectors, light-emitting diodes (LEDs), all-optical logic gates, and transistors.^[2–7] Simultaneously, flexible and wearable smart electronics have been

developing rapidly, resulting in countless functional devices such as flexible solar cells, flexible photodetectors, and bendable batteries.^[8–11] Despite the ever-growing interest in using III–V semiconductor NWs for flexible, wearable, and stretchable (FWS) electronics, it has been extremely challenging to achieve functional flexible devices mainly due to noncrystalline nature of plastics that prevents conventional epitaxial NW growth, and epitaxial growth temperatures beyond what can be tolerated by the flexible substrates.^[12] To overcome these limitations, various complex multistage transfer methods have been proposed where NWs are typically transfer-printed or embedded in a dielectric polymer layer and later peeled off and bonded onto flexible plastic substrates.^[13–16] However, these approaches are not compatible to roll-to-roll processing, which relies on direct deposition on substrate such as plastic, and can provide a high throughput for industrial purposes. In addition, low-cost substrates have been considered critical for III–V device costs.^[17] Furthermore, to the best of our knowledge, there are no reports of in situ growth of GaAs NWs, or even GaAs in general, directly on flexible plastic substrates.

For the growth of NWs, self-catalyzed growth is the most straightforward approach as the seed particle deposition takes place in situ and thus requires no processing steps prior to the growth. In addition, it avoids possible contamination from the foreign seed particles such as the typically used Au nanoparticles.^[18] However, self-catalyzed growth of GaAs NWs (i.e., Ga seeded) typically results only in sparse or stunted growth.^[19–21]


In this report, we present self-catalyzed growth of GaAs NWs and demonstrate monolithic LED directly on flexible plastic substrate. The self-catalyzed growth is shown to result in long and dense GaAs NW forest on the plastic substrates, and electron

V. Khayrudinov, A. Sorokina, T. Koskinen, I. Tittonen, H. Lipsanen, T. Haggren
Department of Electronics and Nanoengineering
Micronova
Aalto University
FI-00076 Espoo, Finland
E-mail: vladislav.khayrudinov@aalto.fi

V. Raj, N. Gagrani, C. Jagadish, H. Hoe Tan, T. Haggren
Department of Electronic Materials Engineering
Research School of Physics
The Australian National University
Canberra ACT 2601, Australia

H. Jiang
Department of Applied Physics
Aalto University
P.O. Box 15100, FI-00076 Espoo, Finland

C. Jagadish, H. Hoe Tan, T. Haggren
Australian Research Council Centre of Excellence for Transformative Meta-Optical Systems
Research School of Physics
The Australian National University
Canberra ACT 2601, Australia

 The ORCID identification number(s) for the author(s) of this article can be found under <https://doi.org/10.1002/adpr.202100311>.

© 2022 The Authors. Advanced Photonics Research published by Wiley-VCH GmbH. This is an open access article under the terms of the Creative Commons Attribution License, which permits use, distribution and reproduction in any medium, provided the original work is properly cited.

DOI: 10.1002/adpr.202100311

microscopy is used to reveal the zinc-blende crystal structure. The GaAs NWs are found to exhibit promising light emission and light-trapping properties. The former is evidenced by strong photoluminescence (PL) even at room temperature (RT) and the latter by characterizing the reflectance, transmittance, and absorptance of the NW forest. The LED structure is demonstrated monolithically on the plastic substrate from the p-type GaAs NWs by only three subsequent deposition steps: Au evaporation as Ohmic contact and TiO₂/ITO depositions as electron-selective contact. As such, the reported NW growth and LED demonstration represent a straightforward pathway to roll-to-roll-compatible NW device fabrication scheme, which is of great importance in the integration of GaAs NWs for various flexible optoelectronic devices.

2. Results and Discussion

Figure 1a shows the image of the sample after the growth. It demonstrates a high degree of flexibility of the substrate as well as high-density NW growth that results in dark-gray color, although originally the polyimide (PI) substrate is bright-yellow. This is attributed to the excellent light-trapping properties of the NWs and, as will be discussed later, very low reflectance and high absorptance in the visible range.

Figure 1b–d shows the scanning electron microscopy (SEM) images of as-grown GaAs NWs on PI. The whole area of the substrates is covered with a continuous interconnected network of NWs that grow in random directions with an average length of 15 μm and an average diameter of 800 nm. **Figure 1c** depicts the flexible PI tape compressed between the SEM clamps. **Figure 1b,d** presents higher magnification micrographs showing high-density NW forest, which clearly indicates that PI is suited

for self-catalyzed GaAs NWs growth. Notably, the density and length of self-catalyzed GaAs NWs are in contrast to earlier reports, where metalorganic vapor phase epitaxy (MOVPE) growth typically results in stunted and sparse NWs.^[19–21] The exact beneficial mechanism of the growth on PI is not examined in this study, while it is believed to be related to surface and interface energies.^[22]

In order to study the crystal structure of the samples, transmission electron microscopy (TEM) measurements were performed (two different NWs shown in **Figure 2a,b**, and additional one in **Figure S1**, Supporting Information). The low- and high-magnification TEM micrographs and the diffraction patterns confirm the crystalline nature of the NWs and correspond to a zinc-blende crystal structure for each NW. Defect planes are observed with [1–10] zone axis as is typical to GaAs NWs (**Figure 2b**). The growth direction was toward [–211] for two of the imaged NWs and [110] for one. Energy-dispersive X-ray spectroscopy (EDX) analysis (**Figure 2c**) shows the presence of Ga and As without additional elements or contamination. The Fe and Cu signals originate from the copper grid and stage used in the TEM measurements.

Optical characterization of the GaAs NWs on PI was performed using micro-PL (scanning near-field optical microscope [SNOM]) and macro-PL in order to verify the optical performance of the samples at RT and low temperature (LT) in a range between 70 and 250 K. Undoped GaAs NWs on PI are characterized with micro-PL in **Figure 3a** to study 1) the PL properties of the intrinsic material, 2) whether any signal is observed from impurities, and 3) to study possible variations in peak wavelength between different NWs. The PL spectra in **Figure 3a** show a typical PL peak of undoped GaAs material corresponding to the electron–hole recombination in the Γ -valley with an energy gap of $E_g = 1.42$ eV that shows a strong emission from the NWs

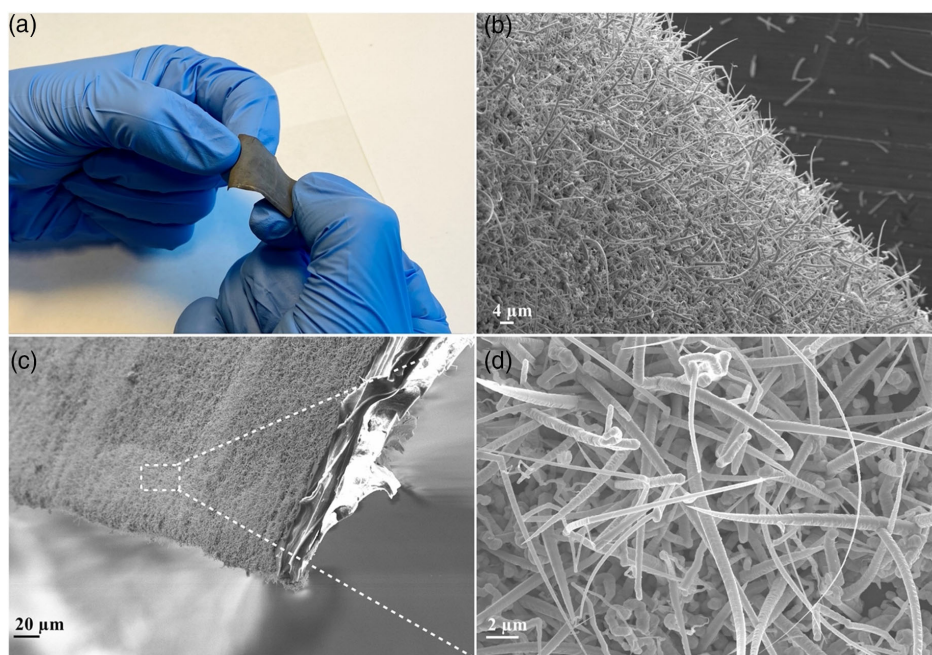


Figure 1. a) Photograph of the GaAs NWs grown directly on flexible PI tape showing a high degree of flexibility. b–d) SEM images of as-grown GaAs NWs directly on flexible PI tape at various magnifications.

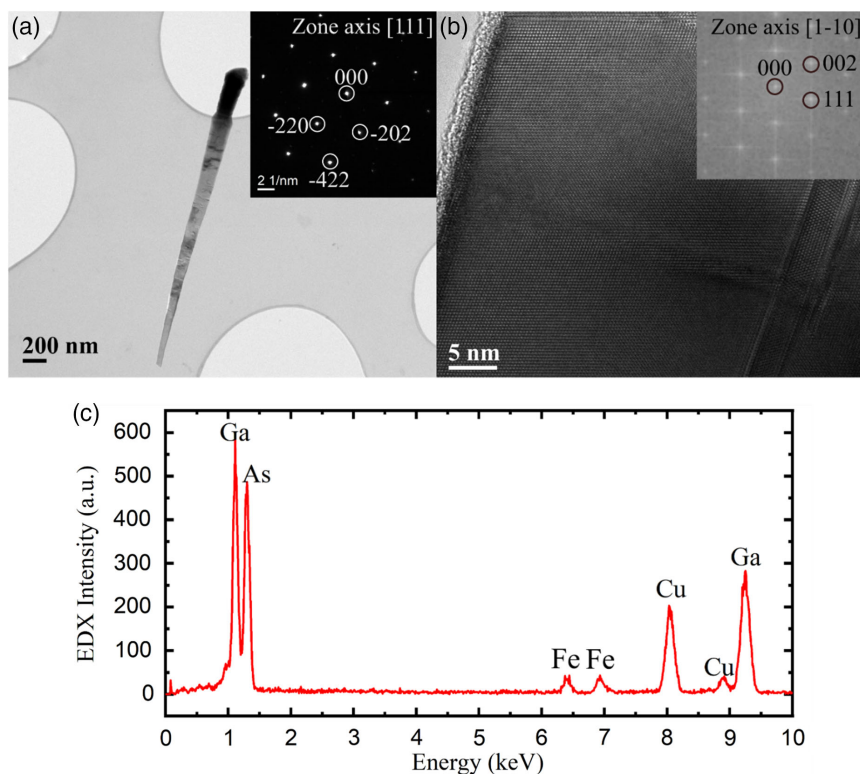


Figure 2. a) Low-magnification TEM image of a typical GaAs NW grown on PI, b) HRTEM image and the corresponding electron diffraction patterns in insets. c) Typical EDX spectrum from the NW.

even at RT. The PL wavelength at GaAs bandgap is indicative of lack of significant amount of impurities in the NWs. Regarding the crystal structure, the micro-PL characterization of several regions revealed PL signal corresponding to ZB crystal only. This is further evidence of predominant ZB crystal structure, as NWs with both wurtzite and ZB have been visible in previous studies with the same setup.^[23] Here, we would also like to note that InP capping layers have been shown to remain stable for several months after initial decrease in PL intensity, in both GaAs NWs and near-surface quantum wells, and therefore, the InP-capped NWs in this study are believed to remain similarly stable.^[24–26]

Figure 3b shows macro-PL spectra from Zn-doped GaAs NWs to study 1) large ensemble of NWs on plastic and 2) doped NWs that are relevant to optoelectronic device structures. The PL peak is redshifted from the peak wavelength of undoped NWs due to Zn doping.^[25] Note that the low-intensity PL tail seen at < 750 nm wavelengths is believed to result from fluorescence from the PI as these wavelengths were observed from a bare PI substrate (Figure S2, Supporting Information) and in addition, they correspond to reported values of active emission from PI.^[27] Emission from the InP passivation is outruled as it would show at longer wavelengths.^[24] GaAs PL peaks in Figure 3b are blueshifted at LT due to the changes of semiconductor bandgap in accordance with Varshni's empirical formula and consistent with the previous optical studies of GaAs NWs.^[28,29] The higher intensity of the peaks at LTs is due to the suppression of nonradiative emission channels at those temperatures.

Figure 4 depicts reflectance, transmittance, and absorbance spectra from bare PI substrate and GaAs NWs on PI. While PI tape without NWs exhibits high *R* and *T*, with the NWs the values of *R* remain at $\approx 10\%$ and *T* well below 10% in the 500–850 nm range. Notably, the NW samples have very high absorbance of 80–90% in the whole visible spectrum which confirms their outstanding light-trapping properties. In fact, the bright-yellow and moderately reflective and transparent PI tape turns dark-gray after NW growth. It should be highlighted here that *R*, *T*, and $1-R-T$ are presented from bare GaAs NWs, while they become clearly less reflective upon deposition of transparent contact material for device purposes (photograph shown in **Figure 5a**). The low reflectance and high absorbance make the GaAs NWs on plastic promising for different NW-based optoelectronic applications. For LEDs, the low reflectance indicates high emittance, or in other words, a large proportion of light generated in the GaAs crystal can escape to the surrounding medium. In addition, low reflectance and high absorbance are critical in achieving high short-circuit current in solar cells and high responsivity in photodetectors.

Finally, we study the electrical properties of Zn-doped p-type GaAs NWs on PI and demonstrate a monolithic LED fabricated directly on the flexible PI substrate. Upon Zn doping, the NWs are found to exhibit Ohmic contact even when measured using metal probes without any contact metal deposition (Figure 5b inset). In contrast, the bare PI substrate is insulating as expected. Similar phenomenon was observed in our previous study, where InAs NWs formed a conductive network between the individual

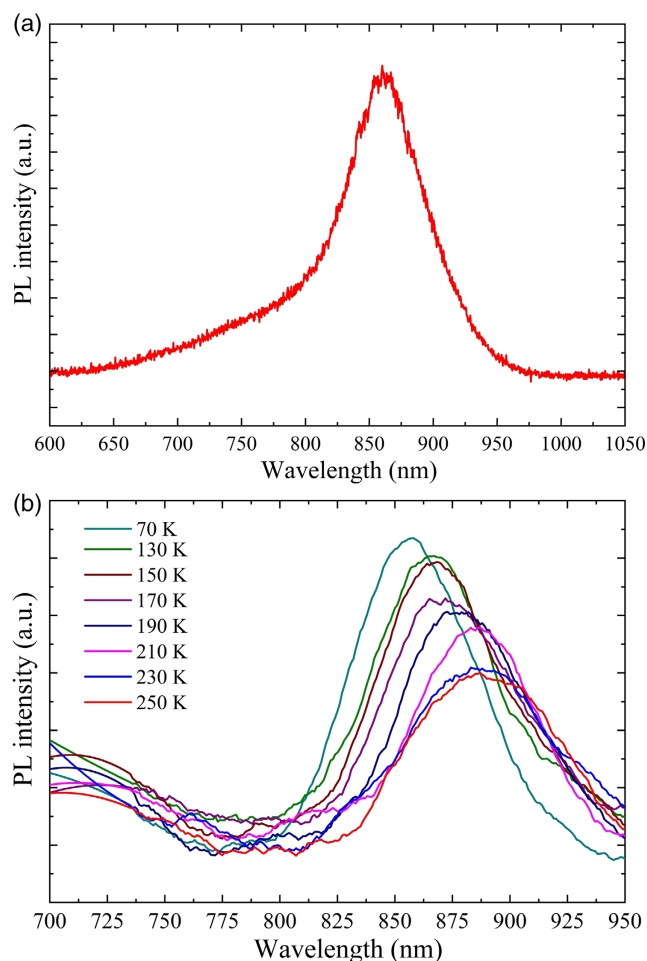


Figure 3. a) Micro-PL measurement of undoped GaAs NWs on flexible PI substrate at RT. b) Temperature dependence of macro-PL spectra of Zn-doped GaAs NWs on PI. The peak wavelength difference close to RT in (a) and (b) results from different doping.

NWs over the whole substrate.^[30] Such Ohmic behavior suggests high doping level, which is further indicated by a redshift in PL emission (Figure 3b). Redshift in PL emission has previously been attributed to high Zn concentration in GaAs NWs.^[31] As a result, it is assumed here that the self-catalyzed NWs are successfully doped and are highly p-type, further indicating the suitability of our NWs for device applications.

To confirm the feasibility of the grown NW forest in flexible device applications, the mechanical flexibility of the GaAs NWs on PI was investigated by controlled bending of the sample to induce tensile stress on the film. Figure S3, Supporting Information, shows the relative change of electrical resistance dR/R_0 when the sample undergoes controlled bending in the tensile direction down to a bending radius of 5.4 mm. At that radius, dR/R_0 shows a 12.6% increase compared to the initial value which is comparable to the previous reports on inorganic flexible materials and surpasses the electrodes based on the ITO/PET film.^[32,33] When the stage is gradually brought back to its original position, the increase in sample resistance is largely reverted, implying that the structure withstands bending well without

showing a clear critical radius. Sample resistance after one bending cycle is 5.5% higher than at the beginning. To further study the mechanical durability of the sample under stress, the same bending cycle was repeated 1000 times. Figure S4, Supporting Information, shows dR/R_0 at both relaxed and bent positions as a function of the number of bending cycles. dR/R_0 at a relaxed position shows a value of $\approx 6.7\%$ after five cycles compared to the initial value, while at the bent position the value is $\approx 12.7\%$. These values stay relatively stable until ≈ 100 cycles, after which the dR/R_0 at both positions starts to show fluctuations likely caused by slight structural damages in the sample. However, dR/R_0 after 1000 cycles is still below 15% for the maximum bending position, signaling that the sample withstands consecutive bending to a great extent.

In order to demonstrate the feasibility of the GaAs NWs on PI for optoelectronic devices, a carrier-selective diode structure was fabricated as shown schematically in Figure 5a. Au was evaporated as a contact metal to the p-GaAs NWs, and in order to form a p–n junction, TiO_2 was deposited as the electron-selective layer followed by ITO deposition over TiO_2 as the n-type contact. This straightforward fabrication scheme results in a diode I – V curve shown in Figure 5b. The choice of these materials is based on the favorable band alignment (simulation by SCAPS-1D is shown in Figure S5, Supporting Information). TiO_2 forms a type-II band alignment with p-GaAs with a small conduction band offset and large valence band offset, significantly reducing the transfer of minority carriers across the junction, thereby acting as a selective contact. Moreover, the majority carrier (holes) become minority carriers at the interface due to band bending induced population inversion, which further reduces the transfer of holes to the contact with ITO/ TiO_2 . Such population inversion has previously been shown to reduce the interface recombination by significantly impeding the flow of one kind of charge carrier. In the presence of ITO/ TiO_2 thin film, a combination of band offset induced selectivity and band bending induced population inversion reduces the recombination current and reverse leakage current leading to improved device characteristics and RT electroluminescence (EL). The device behavior is comparable to previously reported results where the formation of radial junction between selective contact and NW led to substantial improvement in device characteristics.^[34,35]

However, as the materials and deposition conditions were not optimized in the proof-of-concept device here, a significant leakage current is observed in Figure 5b. As discussed above, in ideal scenario the material combination is assumed conducive for high-performance device. Instead, the leakage current is assumed to result predominantly from the device structure and the deposition conditions. First, the TiO_2 deposition by atomic layer deposition (ALD) may have been partially depleted in the top region of the dense NW forest, and thus not covered fully the base region. On the other hand, the ITO was deposited by sputtering which can be approximated as a line-of-sight deposition method. As such, the deposition occurs similarly on the top and base regions of the NWs, thus introducing a leakage channel. Crystal defects and grain boundaries in GaAs may also contribute to the leakage current. Therefore, it is believed that by further material and device optimization would alleviate the leakage current, as suggested by previous reports on carrier-selective contact optimization.^[35–38] We would also like to note here that

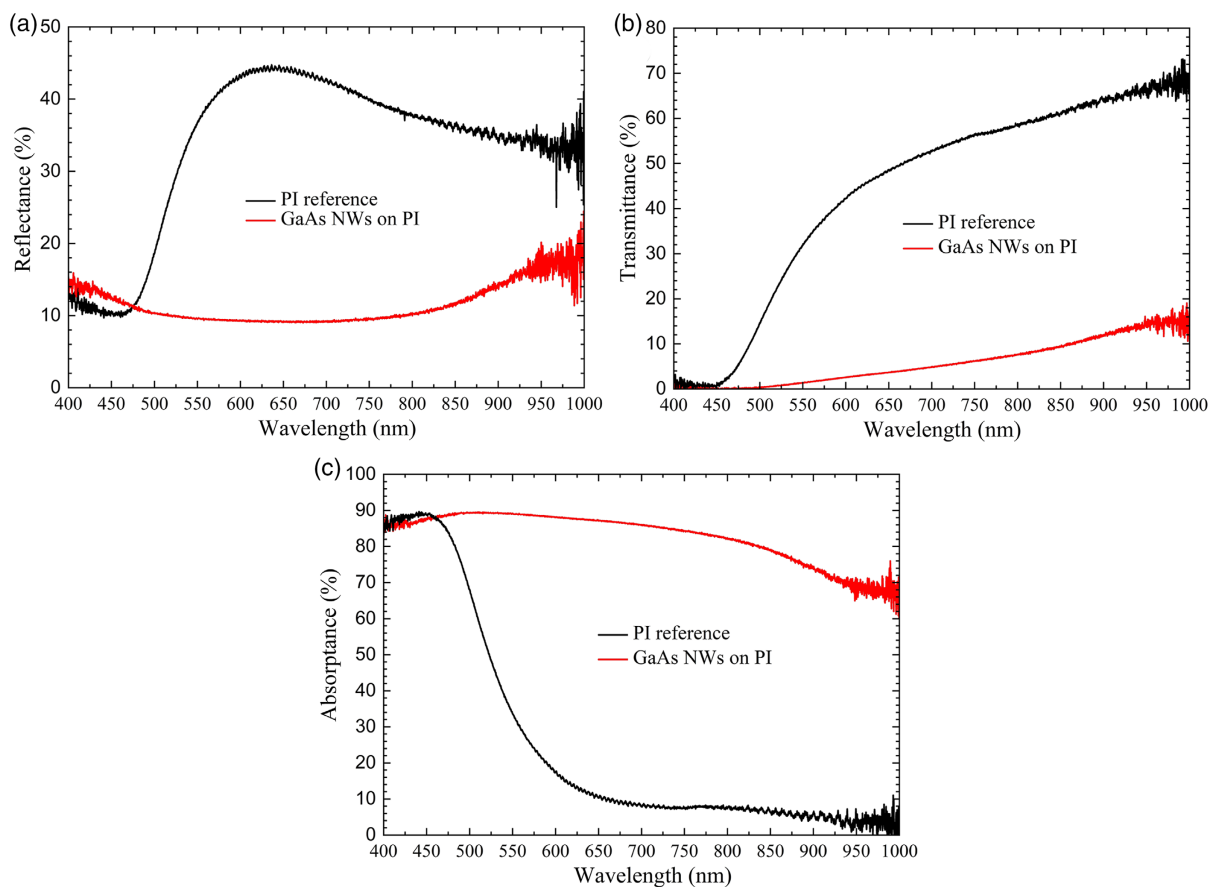


Figure 4. a) Reflectance, b) transmittance, and c) absorbance spectra from bare PI substrate and GaAs NWs grown on PI.

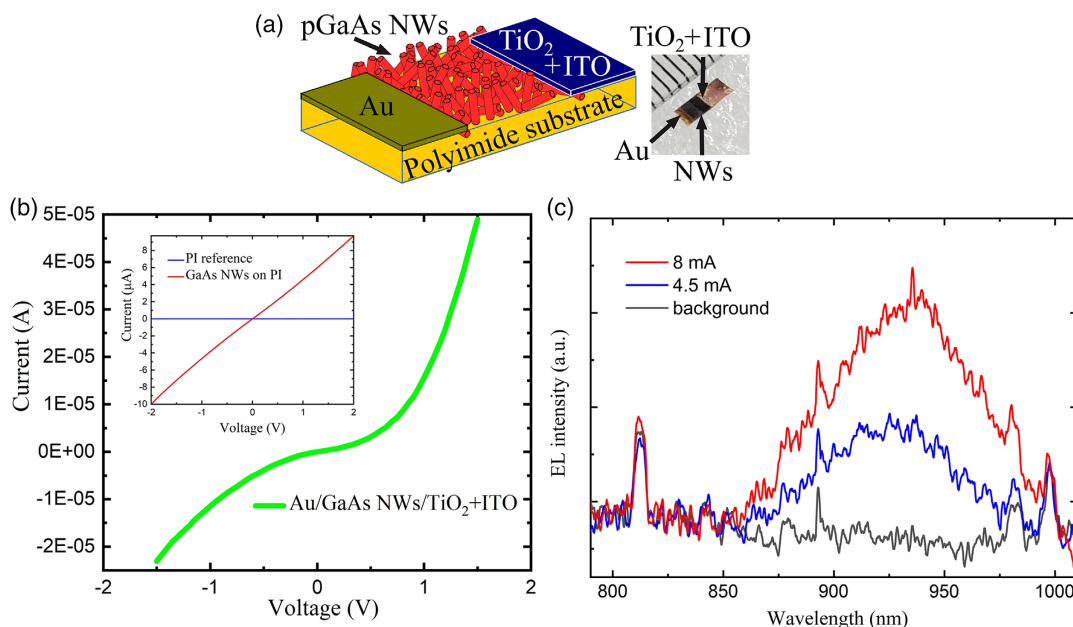


Figure 5. a) Schematic and a photograph of GaAs NW diode structure fabricated monolithically on PI substrate, b) electrical measurements of p-GaAs NWs and the diode structure, and c) EL spectra at RT. In the photograph in (a), the light gray area corresponds to bare p-GaAs NWs and the dark gray area to p-GaAs NWs covered with TiO_2 and ITO. The black lines in the ruler visible in (a) are separated by 1 mm. Note that in (c) the signal is collected from an area of $\approx 175 \mu\text{m}^2$, while the current is spread across a $2 \times 2 \text{ mm}^2$ area of the device.

the LED was fabricated ≈ 3 months after the growth of the NWs, pointing toward a decent stability of the NWs as has been reported before for similarly passivated GaAs structures.^[24]

Despite the moderate diode performance, a clear EL signal at RT was observed with an applied current between the Au and ITO contacts (Figure 5c). We can conclude that a GaAs NW LED was successfully fabricated on flexible PI substrate in only four deposition steps: self-catalyzed NW growth, Au evaporation, TiO₂ deposition, and ITO deposition. The EL signal was observed when applying a current of $\approx 4\text{--}8$ mA; however, it should be noted that the current is spread a $\approx 2 \times 2$ mm² device area while the EL signal is collected only from an area of ≈ 175 μm^2 . Therefore, the current passing through the observed area is orders of magnitude lower than the actual applied current. We also emphasize that the EL signal was initially observed at 900 nm which corresponds to the PL signal from Zn-doped GaAs NWs.^[31] However, after measuring with a drive current of 8–9 mA the peak is shifted to ≈ 940 nm presumably due to heating. We expect that the heating can be mitigated by shortening the distance between the contacts and the junction. The peak at 810 nm is a system artifact.

Regarding the emission profile of the LED structure, individual NWs have tendency to emit toward their long axis.^[39] Here, the NWs are oriented randomly and the far-field emission profile is assumed to be a fairly even distribution over a hemisphere with a reduced emission to angles close to the surface plane (as the emission to these angles is scattered by other NWs). Overall, the LED demonstration shows that the GaAs NWs are conducive for monolithic optoelectronic devices on flexible plastic substrates, and in future, we expect that device performance can still be improved further by optimizing the materials and the device structure. For example, interdigitated and closely spaced contact grids of metal contacts and selective contacts are applicable to the fabrication scheme used here, and would result in 1) increased active device area and 2) significantly reduced resistance between the contacts and the junction area. Thus, they are expected to enable high-efficiency flexible NW solar cells and LEDs. Alternatively, electrically conducting PI is expected to be suitable for GaAs NWs and devices, and it has been shown suitable for InAs NW growth.^[30] Finally, the deposition conditions of the selective contacts may be optimized in future, as well as selective contact materials for GaAs. Bearing in mind that the plastic substrates are extremely low cost and the device fabrication scheme is compatible with the roll-to-roll processing, it is evident that the NWs and the monolithic fabrication on plastic are particularly promising in reducing the cost of III–V optoelectronic devices, while such devices are additionally flexible, expanding their possible application areas.

3. Conclusions

We have shown for the first time the growth and fabrication of GaAs NW LEDs by MOVPE directly on flexible plastic substrates. The NWs were grown in self-catalyzed mode that resulted in a dense forest of long NWs and having a crystalline zinc-blende phase. Good optical quality of the NWs was evidenced by PL emission at RT and light-trapping properties by low reflectance and transmittance. The GaAs NWs were shown to be suitable for

flexible optoelectronics by demonstrating a monolithic LED structure directly on the plastic substrate. The LED was realized in just three subsequent processing steps, i.e., the deposition of Au, TiO₂, and ITO, where TiO₂/ITO acted as an electron-selective contact on p-GaAs NWs. Notably, the direct NW growth on plastic and the proposed device scheme are compatible to high-throughput roll-to-roll processing. Overall, the presented results represent a significant advancement toward flexible, low-cost optoelectronic NW devices and applications.

4. Experimental Section

Self-catalyzed GaAs NWs were grown directly on nonconductive 25 μm -thick PI tape (Polyonics, XT-621) inside a horizontal flow atmospheric pressure MOVPE system. Trimethylgallium (TMGa), tertiarybutylarsene (TBAs), trimethylindium (TMIIn), and tertiarybutylphosphine (TBP) were used as precursors. First, the Ga particles were deposited in situ at 480 °C using TMGa flow of 30.6 $\mu\text{mol min}^{-1}$ for 60 s. Next, GaAs NW growth was started by introducing the TBAs flow (61.20 $\mu\text{mol min}^{-1}$) while maintaining the TMGa flow for 3600 s with the nominal V/III ratio of two. GaAs NWs were doped in situ by introducing a diethylzinc (DEZn) flow at 0.85 $\mu\text{mol min}^{-1}$ during growth. As a last step, GaAs NWs were passivated with InP shell at 530 °C for 3 s with the nominal V/III ratio of 176.^[24] After growth the samples were cooled down under TBP flow. Hydrogen was used as a carrier gas and the total reactor gas flow rate was 5 L min⁻¹. The growth temperatures reported in this work are thermocouple readings of the lamp-heated graphite susceptor, which are slightly higher than the actual substrate surface temperature. Structural properties and morphology of the NWs were studied using SEM (Zeiss Supra 40) operated at 10 keV. High-resolution transmission electron microscopy (HRTEM) measurements were carried out with a JEOL 2200FS double-aberration-corrected field emission gun (FEG) microscope operated at 200 kV. Elemental composition of the NWs was determined using a TEM-integrated EDX tool. The optical characterization of the samples was performed using macro- and micro-PL, reflectance (*R*), and transmittance (*T*) measurements. The absorbance (*A*) was calculated as $A = 1 - R - T$. Macro-PL measurements were done using continuous-wave laser with 532 nm central wavelength and spot size of 100 μm . For PL spectra, a monochromator with a diffraction grating of 600 grooves mm⁻¹ and blazed at 1000 nm, a lock-in amplifier, and a Si photodetector were used. For temperature-dependent measurements, the samples were placed into a closed-cycle liquid He optical cryostat. Micro-PL measurements were performed using a Witec alpha300 SNOM equipped with *cw* 532 nm laser and a Si photodetector. Reflectance and transmittance measurements were obtained using an integrating sphere with a broad light illumination of the samples at 8° and Si photodetector. The NW LEDs were fabricated from Zn-doped p-type NWs with InP capping as a passivation layer. Part of the PI substrate was left intentionally NW-free in order to avoid shorting when applying electrical probes to the contacts. Au (150 nm) was evaporated as Ohmic contact to the NWs using a shadow mask. Next, the substrates were clamped between the glass plates such that the area with Au and a spacing of ≈ 1 mm were covered. On the uncovered area, nominally 15 nm of TiO₂ was deposited with atomic layer deposition followed by a nominally 200 nm of ITO using sputter deposition. TiO₂ was deposited at 120 °C using trimethyltitanium and H₂O as precursors for Ti and O, respectively. An extended purge duration of 8 s was used to ensure highly conformal and uniform deposition of TiO₂. ITO was sputtered at RT with a radio frequency power of 60 W at 1.5 Torr under Ar flow. To measure EL at RT, the current was applied using two probes, and spectra were measured using a charge-coupled device (CCD) (Princeton Instruments, PIXIS) and spectrometer (Acton, SpectraPro 2750). The mechanical flexibility of the samples was studied by a tensile bending experiment, in which a computer-controlled stage was moved back and forth at 0.4 mm increments thus bending the sample placed on the stage, while simultaneously recording the current–voltage characteristics at each stage position.^[40,41] Sample resistance was

computed from a linear fit to the captured I - V curve. The sample for the bending experiment was prepared by e-beam evaporating $8\text{ mm} \times 8\text{ mm}$ Ti/Au ($20\text{ nm}/100\text{ nm}$) contact pads at the ends of the $22\text{ mm} \times 8\text{ mm}$ sample, leaving a $6\text{ mm} \times 8\text{ mm}$ uncoated area in the middle. The sample was then attached onto a supportive PI film with double-sided tape and wiring to the readout electronics was connected on the ends of the contact pads using flexible silver epoxy.

Supporting Information

Supporting Information is available from the Wiley Online Library or from the author.

Acknowledgements

V.K. acknowledges the support of Aalto University Doctoral School, Walter Ahlström Foundation, Elektroniikkainsinöörien Säätiö, Sähköinsinööriiliiton Säätiö, Nokia Foundation, Finnish Foundation for Technology Promotion (Tekniikan Edistämissäätiö), Waldemar von Frenczell's foundation, and Kansallis-Osake-Pankki fund. T.K. acknowledges the support of Aalto University School of Electrical Engineering Doctoral School and the Walter Ahlström Foundation. T.H. acknowledges the support of the Finnish Cultural Foundation and Walter Ahlström Foundation. The Academy of Finland Photonics Flagship PREIN is acknowledged. The authors acknowledge the provision of facilities and technical support by Aalto University at Micronova Nanofabrication Centre. Australian authors acknowledge financial support from the Australian Research Council and facility support from the Australian National Fabrication Facility, ACT node.

Conflict of Interest

The authors declare no conflict of interest.

Data Availability Statement

The data that support the findings of this study are available in the supplementary material of this article.

Keywords

bendable, flexible plastic substrates, GaAs nanowires, light-emitting diodes

Received: October 13, 2021

Revised: March 10, 2022

Published online: March 23, 2022

- [1] E. Barrigón, M. Heurlin, Z. Bi, B. Monemar, L. Samuelson, *Chem. Rev.* **2019**, *119*, 9170.
- [2] G. Otnes, M. T. Borgström, *Nano Today* **2017**, *12*, 31.
- [3] D. Saxena, S. Mokkapat, P. Parkinson, N. Jiang, Q. Gao, H. H. Tan, C. Jagadish, *Nat. Photonics* **2013**, *7*, 963.
- [4] X. Dai, S. Zhang, Z. Wang, G. Adamo, H. Liu, Y. Huang, C. Couteau, C. Soci, *Nano Lett.* **2014**, *14*, 2688.
- [5] K. Tomioka, J. Motohisa, S. Hara, K. Hiruma, T. Fukui, *Nano Lett.* **2010**, *10*, 1639.
- [6] H. Yang, V. Khayrudinov, V. Dhaka, H. Jiang, A. Autere, H. Lipsanen, Z. Sun, H. Jussila, *Sci. Adv.* **2018**, *4*, 7954.
- [7] C. Zhang, X. Miao, K. D. Chabak, X. Li, *J. Phys. D. Appl. Phys.* **2017**, *50*, 393001.
- [8] Kenry, J. C. Yeo, C. T. Lim, *Microsyst. Nanoeng.* **2016**, *2*, 1.
- [9] N. Han, Z. Yang, F. Wang, G. Dong, S. Yip, X. Liang, T. F. Hung, Y. Chen, J. C. Ho, *ACS Appl. Mater. Interfaces* **2015**, *7*, 20454.
- [10] P. Hu, L. Wang, M. Yoon, J. Zhang, W. Feng, X. Wang, Z. Wen, J. C. Idrobo, Y. Miyamoto, D. B. Geohegan, K. Xiao, *Nano Lett.* **2013**, *13*, 1649.
- [11] M. Koo, K.-I. Park, S. H. Lee, M. Suh, D. Y. Jeon, J. W. Choi, K. Kang, K. J. Lee, *Nano Lett.* **2012**, *12*, 4810.
- [12] K. Sakuma, in *Flexible, Wearable, and Stretchable Electronics*, CRC Press, Boca Raton, FL **2020**.
- [13] J. Yoon, S. M. Lee, D. Kang, M. A. Meitl, C. A. Bower, J. A. Rogers, *Adv. Opt. Mater.* **2015**, *3*, 1313.
- [14] J. Valente, T. Godde, Y. Zhang, D. J. Mowbray, H. Liu, *Nano Lett.* **2018**, *18*, 4206.
- [15] N. Guan, X. Dai, A. V. Babichev, F. H. Julien, M. Tchernycheva, *Chem. Sci.* **2017**, *8*, 7904.
- [16] M. Tchernycheva, N. Guan, X. Dai, A. Messanvi, H. Zhang, F. Bayle, V. Neplokh, V. Piazza, F. H. Julien, C. Bougerol, M. Vallo, C. Durand, J. Eymery, in *Materials and Devices Conference, NMDC 2016 – Conf. Proc.*, IEEE, Piscataway, NJ **2016**.
- [17] V. Raj, T. Haggren, W. W. Wong, H. H. Tan, C. Jagadish, *J. Phys. D. Appl. Phys.* **2022**, *55*, 143002.
- [18] Z. Dong, Y. André, V. G. Dubrovskii, C. Bougerol, C. Leroux, M. R. Ramdani, G. Monier, A. Trassoudaine, D. Castelluci, E. Gil, *Nanotechnology* **2017**, *28*, 125602.
- [19] J. Lohani, S. Sapra, R. Tyagi, *Vacuum* **2019**, *164*, 343.
- [20] J. Lohani, R. K. Bag, M. V. G. Padmavati, S. Sapra, R. Tyagi, *Chem. Phys.* **2017**, *493*, 175.
- [21] S. Breuer, F. Karouta, H. H. Tan, C. Jagadish, in *Conf. on Optoelectronic and Microelectronic Materials and Devices, Proc.s, COMMAD MOCVD growth of GaAs nanowires using Ga droplets*, **2012**, p. 39 <https://doi.org/10.1109/COMMAD.2012.6472349>.
- [22] H. J. Joyce, Q. Gao, H. H. Tan, C. Jagadish, Y. Kim, J. Zou, L. M. Smith, H. E. Jackson, J. M. Yarrison-rice, P. Parkinson, M. B. Johnston, *Prog. Quantum Electron.* **2011**, *35*, 23.
- [23] T. Haggren, N. Anttu, H. Mäntynen, C. Tossi, M. Kim, V. Khayrudinov, H. Lipsanen, *Nanotechnol.* **2020**, *31*, 384003.
- [24] T. Haggren, H. Jiang, J. P. Kakko, T. Huhtio, V. Dhaka, E. Kauppinen, H. Lipsanen, *Appl. Phys. Lett.* **2014**, *105*, 33114.
- [25] H. Lipsanen, M. Sopanen, M. Taskinen, *Cite as Appl. Phys. Lett.* **1996**, *68*, 2216.
- [26] A. Aierken, T. Hakkarainen, J. Tiilikainen, M. Mattila, J. Riikonen, M. Sopanen, H. Lipsanen, *J. Cryst. Growth* **2007**, *309*, 18.
- [27] S. Konde, J. Ornik, J. A. Prume, J. Taiber, M. Koch, *Mar. Pollut. Bull.* **2020**, *159*, 111475.
- [28] Y. P. Varshni, *Physica* **1967**, *34*, 149.
- [29] L. V. Titova, T. B. Hoang, H. E. Jackson, L. M. Smith, J. M. Yarrison-Rice, Y. Kim, H. J. Joyce, H. H. Tan, C. Jagadish, *Appl. Phys. Lett.* **2006**, *89*, 173126.
- [30] V. Khayrudinov, M. Remennyi, V. Raj, P. Alekseev, B. Matveev, H. Lipsanen, T. Haggren, *ACS Nano* **2020**, *14*, 7484.
- [31] T. Haggren, J. P. Kakko, H. Jiang, V. Dhaka, T. Huhtio, H. Lipsanen, in *Proceedings of the IEEE Conference on Nanotechnology*, IEEE, Piscataway, NJ **2014**, p. 825.
- [32] J. Coroa, B. M. Morais Faustino, A. Marques, C. Bianchi, T. Koskinen, T. Juntunen, I. Tittunen, I. Ferreira, *RSC Adv.* **2019**, *9*, 35384.
- [33] M. Song, D. S. You, K. Lim, S. Park, S. Jung, C. S. Kim, D. H. Kim, D. G. Kim, J. K. Kim, J. Park, Y. C. Kang, J. Heo, S. H. Jin, J. H. Park, J. W. Kang, *Adv. Funct. Mater.* **2013**, *23*, 4177.
- [34] V. Raj, K. Vora, L. Fu, H. H. Tan, C. Jagadish, *ACS Nano* **2019**, *13*, 12015.
- [35] V. Raj, H. H. Tan, C. Jagadish, *Appl. Mater. Today* **2020**, *18*, 100503.

- [36] V. Raj, T. Haggren, J. Tournet, H. H. Tan, C. Jagadish, *ACS Appl. Energy Mater.* **2021**, *4*, 1356.
- [37] P. R. Narangari, S. K. Karuturi, Y. Wu, J. Wong-Leung, K. Vora, M. Lysevych, Y. Wan, H. H. Tan, C. Jagadish, S. Mokkaapati, *Nanoscale* **2019**, *11*, 7497.
- [38] X. Yin, C. Battaglia, Y. Lin, K. Chen, M. Hettick, M. Zheng, C. Y. Chen, D. Kiriya, A. Javey, *ACS Photonics* **2014**, *1*, 1245.
- [39] G. Grzela, R. Paniagua-Domínguez, T. Barten, Y. Fontana, J. A. Sánchez-Gil, J. Gómez Rivas, *Nano Lett.* **2012**, *12*, 5481.
- [40] S. Il Park, J. H. Ahn, X. Feng, S. Wang, Y. Huang, J. A. Rogers, *Adv. Funct. Mater.* **2008**, *18*, 2673.
- [41] T. Juntunen, H. Jussila, M. Ruoho, S. Liu, G. Hu, T. Albrow-Owen, L. W. T. Ng, R. C. T. Howe, T. Hasan, Z. Sun, I. Tittonen, *Adv. Funct. Mater.* **2018**, *28*, 1800480.